

BRIEF COMMUNICATIONS

ASYMMETRY CURRENTS AND ADMITTANCE IN SQUID AXONS

H. M. FISHMAN, AND L. E. MOORE, *Department of Physiology and Biophysics,
University of Texas Medical Branch, Galveston, Texas 77550 and The
Marine Biological Laboratory, Woods Hole, Massachusetts 02543 U.S.A.*
AND

D. POUSSART, *Department of Electrical Engineering, Université Laval,
Québec, Canada*

ABSTRACT The complex admittance of squid (*Loligo pealei*) axon was measured rapidly (within 1 s) with pseudo-random small signals and discrete Fourier transform techniques under guarded, "space-clamp" conditions and during suppression of ion conduction. Asymmetry currents were measured by paired step clamp pulses of ± 70 mV from a holding potential of -97 mV and gave an apparent capacitance of $0.36 \mu\text{F}/\text{cm}^2$. However, the admittance data showed no change in capacitance at holding potentials from -97 to -67 mV and gave a decrease of 0.07 to $0.15 \mu\text{F}/\text{cm}^2$ at -37 mV. The failure to observe a capacitance increase at low membrane potentials suggests the following possibilities: (a) the asymmetry current is a displacement current that inactivates completely with time, and (b) the asymmetry current is not a displacement current and arises from large signal effects (i.e., delayed nonlinearity in ionic current) on the membrane.

Time domain measurement of a displacement-like asymmetry current after suppression of the usual voltage-dependent ion conduction processes in excitable membranes has generated considerable interest (1, 2). One interpretation of these currents is that they are a manifestation of the movement of membrane-bound charges associated with the opening and closing ("gating") of ion channels. A recent review (3) summarizes the evidence for this point of view.

Frequency domain analysis is an alternative and widely used approach in describing dielectric phenomena. Recently, an instrument for measuring transfer functions in real-time has been developed by using pseudo-random signals and discrete Fourier transform techniques (4, 5). This report (6) describes the results of application of this method to measure the complex admittance of squid axon under the same conditions in which asymmetry currents are measured.

Squid (*Loligo pealei*) axons were voltage-clamped with an internal axial "piggyback" electrode with an external potential reference electrode, as described previously (7),

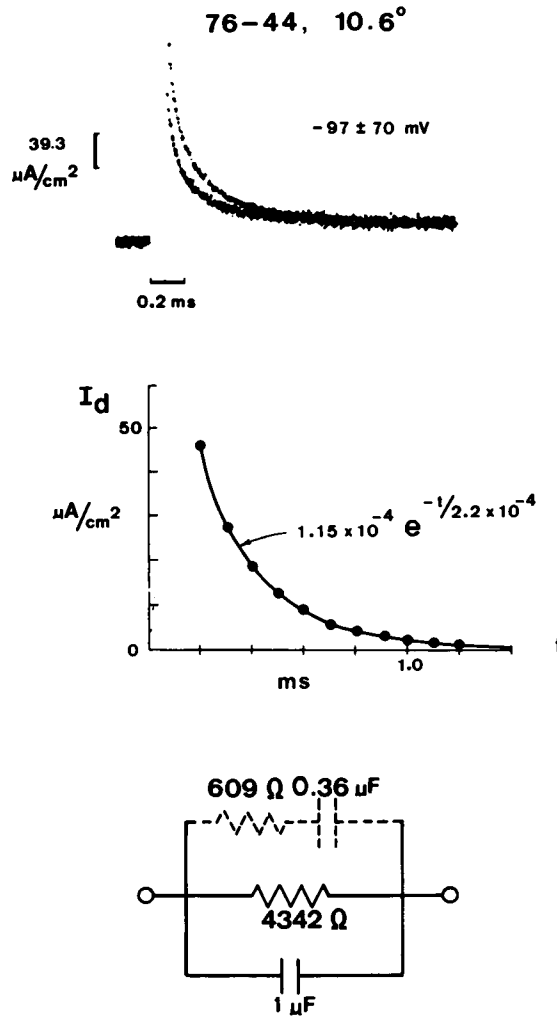


FIGURE 1 (Upper) Current response of a squid axon (under suppressed ion conduction conditions) to a single depolarizing step (+70 mV) and a single hyperpolarizing step (-70 mV) from a holding potential of -97 mV. (Middle) Asymmetry current (filled circles) obtained by subtraction of currents in the upper records. Solid curve is the function indicated. (Lower) The dashed branch, in parallel with leakage and static capacitance, accounts for the asymmetry current. The element values are for 1 cm² of membrane.

and external platinized platinum plates for current collection and guards. Axons were internally perfused with a solution of 290 mM CsF buffered to pH 7.4 at 22°C with Tris-HCl and with 400 mM sucrose added to match the osmolarity of the external solution. The external solution was either artificial sea water (ASW), consisting of 423 mM NaCl, 9 mM KCl, 9.3 mM CaCl₂, 23 mM MgCl₂, 25.5 mM MgSO₄, 5 mM Tris-HCl, and 1 μM tetrodotoxin (TTX), or a Na and K-free ASW containing TTX in which Tris-HCl replaced the NaCl and KCl.

Before the admittance measurements, an asymmetry or difference current was always measured in step voltage clamp by holding the membrane potential at -97 mV and applying a pair of pulses to move the membrane potential ± 70 mV from the holding potential. Fig. 1 (uppermost portion) shows the current-time record for a single depolarizing pulse (applied to the noninverting input of a differential amplifier) and the inverted current record for a single hyperpolarizing pulse (applied to the inverting input of the same differential amplifier). The filled circles in the graph of I_d with time in Fig. 1 were obtained by taking the difference between the upper current records at various times. The solid curve is a fit of the filled circles by a single exponential function shown in the figure. The difference current is modeled as a series resistance-capacitance (RC) branch, (dashed in Fig. 1) with the value of R ($609 \Omega \cdot \text{cm}^2$) obtained from the exponential function at $t = 0$ and the step of 70 mV. The apparent capacitance C is obtained from the time constant (0.22 ms) and the determined value of R . The apparent capacitance is in agreement with those obtained by others (1, 2). A parallel "leakage" resistance of $4342 \Omega \cdot \text{cm}^2$ was calculated from the steady level of current after the decay in the uppermost records in response to the ± 70 mV steps. A static capacitance of $1 \mu\text{F}/\text{cm}^2$ is also assumed. From this circuit description the complex admittance was calculated with and without a series resistance of $10 \Omega \cdot \text{cm}^2$. Fig. 2 shows calculations of the magnitude and phase functions of the admittance for the circuit representation of the measurement. It is quite clear from Fig. 2 that the addition of the RC branch to the circuit produces a significant change, which should be measurable in the steady state, in both the magnitude and phase of admittance. That is, the $|Y|$ and ϕ curves without the RC branch correspond to an admittance measurement with the membrane potential held at hyperpolarized value (membrane charge is not translocated in response to small-signal voltage perturbations), whereas the curves with the RC branch included correspond to an admittance measurement at some depolarized membrane potential (where membrane charge is translocatable in response to small signal perturbations and thus contributes to capacitance).

In contrast to more conventional techniques, the method used in these experiments to measure the complex admittance of squid axon has as its main attribute the efficient use of experimental time, with speed near the theoretical limit for time-frequency domain analysis (4, 5). A description of the measurement procedure follows. Details of the implementation of the method are also described in Refs. 4 and 5. The membrane potential is initially clamped to a selected holding potential, to which a small (2 mV peak-to-peak) pseudo-random binary sequence (PRBS) is superposed without gaps between successive PRBS periods. When a measurement is to occur, a sequencer issues the request for a step pulse of chosen polarity and amplitude. The request occurs at a time before the next complete PRBS period. The duration of the lead time, typically 100 – 200 ms, is chosen so that the total membrane current response, I_m , will be in a "steady state" when the forthcoming period occurs. In the meantime, an analogue switch maintains the input of the processor, which computes the discrete Fourier transform (DFT), at ground potential to prevent transient overloading. I_m undergoes its time-course with a small pseudo-random component that carries the

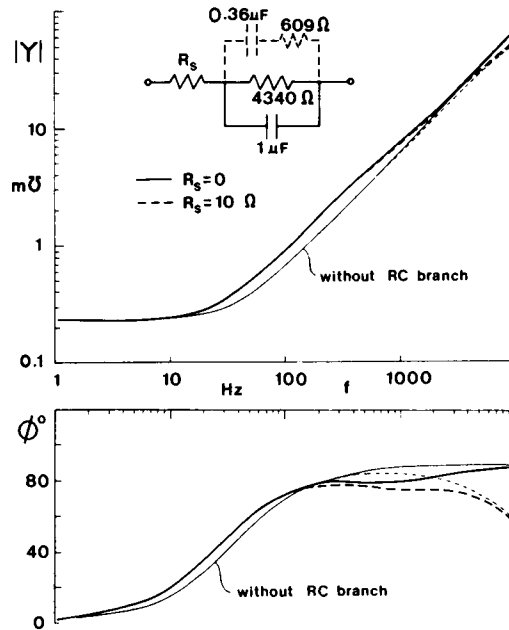


FIGURE 2 Calculated complex admittance of the circuit (inset) which models membrane asymmetry current, with and without a series resistance, R_s . The magnitude and phase functions without the dashed RC branch correspond to the admittance which should be measured at a large negative holding potential, and with the RC branch correspond to the admittance which should be measured at a low membrane potential.

admittance information, which must be extracted. At a time (e.g., 80 ms), also selected so that the general response is in a steady state, I_M is sampled and that value is held in memory by a sample-and-hold circuit. Sampling is preceded by low-pass filtering (dual RC network, time constant = 0.68 ms) for rejection of the pseudo-random spikes which reflect dominance of the membrane capacity at high frequency. In conjunction with the nearly zero mean property of linear PRBS signals, the filtering insures that the DC value in memory is well centered within the dynamic excursions of the response. A differential amplifier subtracts this DC value from I_m . Immediately after the sampling transients have subsided, the analogue switch closes and the pseudo-random response component, now superposed on a minimal pedestal, is applied to the input of the DFT processor. This automatic restoration of DC base line allows full utilization of the dynamic range of the DFT processor. Precisely when the new PRBS period is beginning, the synchronization circuits, contained within the instrument (4,5), initiate sampling and storage in the input memory. Immediately after completion of the period (which lasts from 100 ms to 10 s, depending on the selected frequency range) the system is reset to rest condition. Within 100 ms, the magnitude and phase of the admittance, corresponding to membrane potential of holding potential plus step value, is computed, displayed, and available for plotting. This paradigm insures that the

duration of the perturbation away from the holding potential is nearly as short as the frequency resolution of the recorded admittance data allows.

Fig. 3 shows measured admittance data in the frequency range 10–1,000 Hz, which is typical of data from 12 axons. Each set of magnitude and phase data is acquired over a measurement period of 250 ms and within approximately 1 s of the onset of the change of potential, as described above. It is clear that the expected behavior in Fig. 2 is not observed. In addition, there are two notable features. First, an extrapolation of the $|Y|$ to zero frequency yields a potential-dependent conductance. The DC conductance change with voltage also results in a shift of the phase curves and makes a direct comparison of the curves difficult. Secondly, at frequencies above 200 Hz, where the admittance behavior is dominated by the effective circuit capacitance, a small shift downward is observed in the $|Y|$ at a depolarized potential of -20 mV. This downward shift at depolarized potentials in $|Y|$ at high frequency is a reproducible effect and corresponds to a decrease in capacitance of $0.07 \mu\text{F}/\text{cm}^2$ to a maximum of $0.15 \mu\text{F}/\text{cm}^2$ shown in Fig. 4, measured from the same axon used to obtain the data in Fig. 1. The data in Fig. 4 show no change in capacitance for holding potentials in the range -100 to -65 mV, not the expected result based on previous reports (8,9) of asymmetry currents. Takashima (10), using an admittance bridge, also reports that after suppression of ion conduction, the effective capacitance was independent of holding potential. In addition, he did not observe a capacitance change measured at a

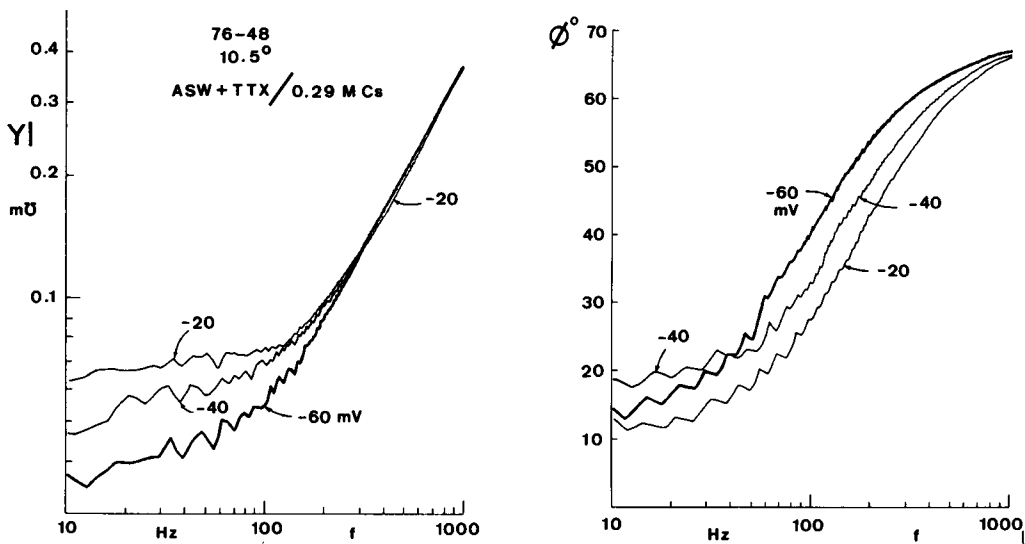


FIGURE 3 Complex admittance of a squid axon measured under suppressed ion conduction conditions and at the indicated holding potentials. See text for details of the admittance measurement. Note: changes in $|Y|$ at low frequency with potential and changes calculated in Fig. 2 are not observed. The resolution of the magnitude measurement in the asymptote region (above 300 Hz), where the signal-to-noise ratio is excellent, is $1\text{--}2\%$.

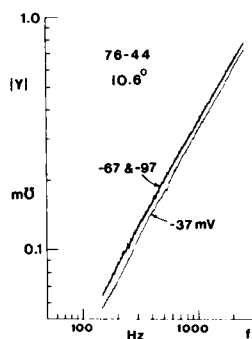


FIGURE 4 Conditions similar to Fig. 3 but in the frequency range where capacitance dominates admittance. Note in $|Y|$ no change in capacitance between -67 and -97 mV and a decrease (shift downward) in capacitance at -37 mV. Axon area in both Figs. 3 and 4 is about 0.06 cm^2 .

single frequency within 10 ms after a step change from a hyperpolarized to a depolarized membrane potential.

The apparent contradiction between time and frequency domain measurements does not lie in the differences between the two types of measurements. Recent experiments (11), in which field-induced movements of tetraphenylborate ions across a lipid bilayer modeled the amplitude and time-course of asymmetry currents in nerve (8, 9), gave a capacitance change in admittance measurements that agreed with the charge movement obtained from step potential measurements. The failure to find a correspondence between an assumed charge movement associated with asymmetry currents and capacitance change in admittance measurements in these experiments suggests the following possibilities: (a) the asymmetry current is a displacement current that inactivates completely with time, (b) the asymmetry current is not a displacement current and arises from large signal effects (i.e., delayed, nonlinearity in ionic current) on the membrane. With respect to (a), it is significant that a capacitance *decrease* is observed (Fig. 4, -37 mV) in admittance. It is conceivable that a portion of the difference current is associated with a voltage-dependent desorption of (non)-specific surface charge, which may or may not be associated with ion channel gating. To our knowledge, desorption models have not been explored as a possible explanation of asymmetry currents, and therefore cannot be excluded at this time. Electrostriction (12) is another phenomenon that could produce a capacitance decrease unrelated to channel gating. Finally, with respect to possibility b, the admittance data show a clear potential dependence in the residual (leakage) conductance in the steady state (1 s), which suggests that a significant portion of the difference current could be associated with a delayed (nonlinear?) ionic current. Although an ionic current through leakage channels would have to have peculiar properties (such as the proper time and voltage dependence as well as subjection to chemical agents and inactivation by depolarization), such properties are not inconceivable since slight changes in slope conductance were observed (13) in early "instantaneous" current-voltage relations in axons treated with

TTX and tetraethylammonium ion and the present data on leakage are not adequate to exclude this possibility.

We thank Dr. Ronald Grisell for discussions and assistance and Mr. Paul Sawyer for computer programming.

This work was supported in part by National Institutes of Health grant NS 11764 (HMF), NS 13520 (LEM) and Canadian National Research Council grant A 5274 (DP).

Received for publication 22 March 1977.

REFERENCES

1. ARMSTRONG, C. M., and F. BEZANILLA. 1974. Charge movement associated with the opening and closing of the activation gates of the Na channels. *J. Gen. Physiol.* **63**:533-552.
2. KEYNES, R. D., and E. ROJAS. 1974. Kinetics and steady-state properties of the charged system controlling sodium conductance in the squid giant axon. *J. Physiol. (Lond)*. **239**:393-434.
3. MEVES, H. 1977. Activation, inactivation and chemical blockage of the gating current in squid giant axons. *Ann. N.Y. Acad. Sci.* In press.
4. POUSSART, D., and U. S. GANGULY. 1977. Rapid measurement of system kinetics. An instrument for real-time transfer function analysis. *Proc. IEEE (Inst. Electron. Electr. Eng.)*. **65**:741-746.
5. POUSSART, D., L. E. MOORE, and H. M. FISHMAN. 1977. Ion movements and kinetics in squid axon. I. Complex admittance. *Ann. N.Y. Acad. Sci.* In press.
6. FISHMAN, H. M., L. E. MOORE, and D. POUSSART. 1977. Charge movements and admittance in squid axon. *Biophys. J.* **17**:11a. (Abstr.).
7. FISHMAN, H. M., D. POUSSART, L. E. MOORE, and E. SIEBENGA. 1977. K conduction description from the low frequency impedance and admittance of squid axon. *J. Memb. Biol.* **32**:255-290.
8. KEYNES, R. D., E. ROJAS, and B. RUDY. 1974. Demonstration of a first-order voltage-dependent transition of the sodium activation gates. *J. Physiol. (Lond)*. **239**:100-101P.
9. MEVES, H. 1974. The effect of holding potential on the asymmetry currents in squid giant axons. *J. Physiol. (Lond.)*. **243**:847-867.
10. TAKASHIMA, S. 1977. Voltage-development membrane capacity of squid axon. *Ann. N.Y. Acad. Sci.* In press.
11. SZABO, G. 1977. Admittance and step-clamp response for ion redistribution in bilayers: a simple model for gating currents. *Biophys. J.* **17**:11a. (Abstr.).
12. BLATT, F. J. 1977. Gating currents. The role of nonlinear capacitive currents of electrostrictive origin. *Biophys. J.* **17**:43-52.
13. FISHMAN, H. M. 1970. Leakage current in the squid axon membrane after application of TTX and TEA. *Biophys. J.* **10**:109a. (Abstr.).